



Cite this: DOI: 10.1039/d4na00569d

## Recent progress in carbon nanomaterials for highly flexible fibrous aqueous zinc-ion batteries

Guoqing Lu,<sup>ab</sup> Qiqing Xi,<sup>c</sup> Yanyan Shao,<sup>d</sup> Yinan Yang,<sup>b</sup> Yichuan Rui<sup>id</sup> \*<sup>a</sup>  
and Yuanlong Shao<sup>id</sup> \*<sup>b</sup>

Fibrous zinc-ion batteries (FZIBs) are ideal wearable energy storage devices with unparalleled utility in the next generation of flexible electronics. However, the conventional electrode materials still present challenges to achieve both good electrochemical performance and mechanical deformability. This hinders their large-scale production and commercial application. Carbon nanomaterials exhibit a number of advantageous properties, including high chemical stability, high conductivity, low cost, and high mechanical flexibility. These characteristics make them an attractive option for modifying electrode materials. This review presents an overview of the latest research developments and practical applications of carbon nanomaterial-assisted FZIBs cathodes and anodes. It also identifies the key challenges currently limiting the performance of high-performance FZIBs and outlines potential future research directions.

Received 12th July 2024  
Accepted 13th September 2024

DOI: 10.1039/d4na00569d

rsc.li/nanoscale-advances

### 1. Introduction

In recent years, the rapid development of flexible wearable devices, including smart clothing, implantable medical devices and artificial electronic skin, has rendered traditional energy storage devices increasingly unable to meet the practical application requirements of wearable and implantable devices.<sup>1</sup> Consequently, the development of high-performance, high-safety flexible energy storage devices is of particular importance.<sup>2</sup> Flexible batteries are portable energy storage devices that are widely utilized in wearable electronics and smart textiles due to their good wearability and high adaptability.<sup>3</sup> Nevertheless, the commercial application of flexible batteries is not yet fully developed,<sup>4</sup> as the current battery system presents significant challenges in terms of flexibility and safety. Consequently, the development of flexible batteries with high electrochemical performance, great mechanical properties and safety is of paramount importance to ensure their successful manufacture and application.<sup>5</sup> Flexible fibrous batteries exhibit excellent mechanical properties, including the ability to withstand bending, twisting, and stretching in multiple directions.<sup>6</sup> Additionally, they are highly compatible with the current textile

industry. It is anticipated that this will become the principal avenue of development for flexible batteries in the future.<sup>7</sup> Flexible fibrous batteries manifest a flexible structural design and unique textile system integration capabilities, which collectively offer promising prospects for the development of multifunctional integrated systems.<sup>8</sup> Zinc-ion batteries (ZIBs) exhibit a number of significant advantages, including high safety, a high theoretical capacity (820 mA h g<sup>-1</sup>, 5855 mA h cm<sup>-3</sup>), a low redox potential (−0.76 V vs. SHE (standard hydrogen electrode)), higher ionic conductivity and mobility of the aqueous electrolyte,<sup>9,10</sup> environmental friendliness, a lower cost and a superior safety profile compared to lithium-ion batteries.<sup>11</sup> Although lithium-ion batteries present the advantages of high energy density and long cycle life, they also suffer from disadvantages of the increasing cost of lithium mineral and safety issues.<sup>12</sup> The electrolyte used in lithium-ion batteries demonstrates inherent flammable and explosive characteristics, which can easily cause the battery to burn or explode. This potential safety hazard has resulted in the limited utilization of lithium-ion batteries.<sup>13–15</sup>

For ZIBs, the conventional metal oxide cathodes, such as manganese-based and vanadium-based materials,<sup>16,17</sup> are unable to achieve fast electron transfer due to their inherent low conductivity. During the charging and discharging process, as ions are continuously inserted and extracted, the cathode material will undergo gradual volume changes and dissolution.<sup>18</sup> Prussian blue analogues (PBAs) and organic compounds are also frequently employed as cathode materials for FZIBs.<sup>19</sup> However, both have the disadvantage of rapid capacity attenuation during cycling, which hinders their further development. FZIBs commonly employ metal Zn wire as the anode. The

<sup>a</sup>School of Chemistry and Chemical Engineering, Shanghai University of Engineering Science, Shanghai 201620, China. E-mail: ryc713@126.com

<sup>b</sup>School of Materials Science and Engineering, Peking University, Beijing 100871, China. E-mail: shaoyuanlong@pku.edu.cn

<sup>c</sup>School of Materials Science and Engineering, Shanghai University of Engineering Science, Shanghai 201620, China

<sup>d</sup>College of Energy Soochow Institute for Energy and Materials Innovations (SIEMIS), Key Laboratory of Advanced Carbon Materials and Wearable Energy Technologies of Jiangsu Province, Soochow University, Suzhou, 215006, China



natural abundance of zinc in the environment contributes to reducing production costs. However, the hydrogen evolution reaction (HER), dendrite growth and corrosion inherent in zinc anodes can cause rapid capacity attenuation, gas generation, short circuits and other undesirable side-reactions, ultimately leading to rapid battery failure.<sup>20,21</sup>

Therefore, the principal strategy for enhancing the overall performance of FZIBs is to optimize the structure of the cathode and anode materials.<sup>22,23</sup> Among the electrode modification materials that have been developed, carbon nanomaterials have unique advantages.<sup>24,25</sup> Carbon nanomaterials encompass a diverse range of materials, including carbon quantum dots (CDs), graphene oxide (GO), carbon nanotubes (CNTs) and their derivatives. These materials exhibit a multitude of distinct physical and chemical properties,<sup>26,27</sup> as shown in Fig. 1. The exceptional electrical conductivity of carbon nanomaterials,<sup>28,29</sup> such as CNTs, renders them ideal for use as conductive substrates or three-dimensional networks for cathodes. This improves the efficiency of electron transport and inhibits the dissolution of electrode materials.<sup>30,31</sup> The use of carbon nanomaterials as anode substrates can facilitate the deposition of zinc, with regulation of the zinc ion ( $\text{Zn}^{2+}$ ) deposition behavior.<sup>32,33</sup> The construction of an interface coating can prevent the electrolyte from directly coming into contact with the zinc metal anode, thereby reducing the occurrence of interfacial side reactions.<sup>34</sup> The use of carbon nanomaterials as electrolyte additives can result in the even distribution of

electric fields on the surface of the zinc anode, thereby inhibiting dendrite growth,<sup>35</sup> which further alleviates the inherent problems associated with the hydrogen evolution reaction (HER) and corrosion. For the fields of artificial intelligence and smart textiles, it is of paramount importance to provide a comprehensive overview of the most recent advancements in FZIBs. As summarized in Fig. 2, in the past decade, various multifunctional carbon nanomaterials have been widely employed as cathode and anode materials for FZIBs.<sup>36–47</sup> The majority of the published review articles to date have concentrated on the utilization of carbon nanomaterials in aqueous  $\text{Zn}^{2+}$  batteries.<sup>48–50</sup> This article will comprehensively summarize the mechanism of carbon nanomaterials in fiber-shaped batteries, providing an in-depth analysis of the application challenges and future development directions.

## 2. Charge storage mechanism and structural design of FZIBs

### 2.1 Operation principles

The discharge/charge process of FZIBs is primarily dependent on the reversible transport of  $\text{Zn}^{2+}$  in the electrolyte between the anode and cathode. During the discharge process, the zinc anode releases  $\text{Zn}^{2+}$  into the electrolyte, which then migrates to the cathode.<sup>51–53</sup> The zinc anode undergoes an oxidation reaction, resulting in the release of electrons and the production of  $\text{Zn}^{2+}$ . The cathode material (*e.g.*, manganese oxide, vanadium

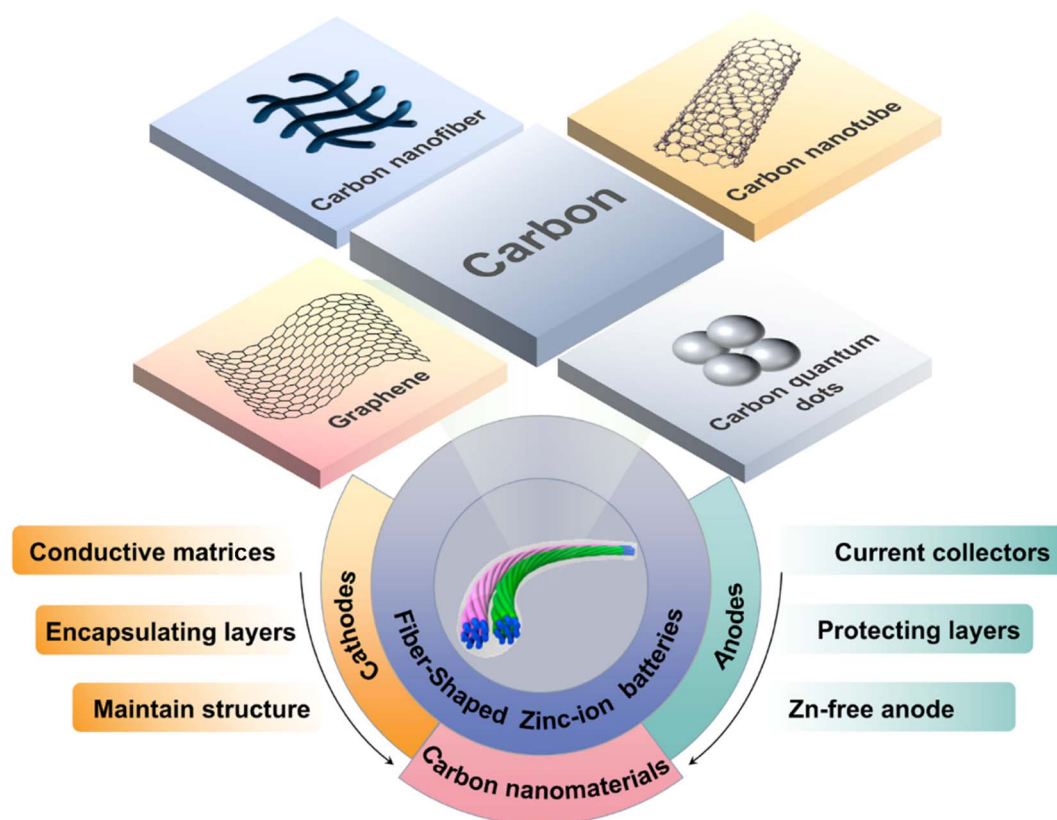


Fig. 1 Diagram of the important role of carbon nanomaterials in FZIBs.



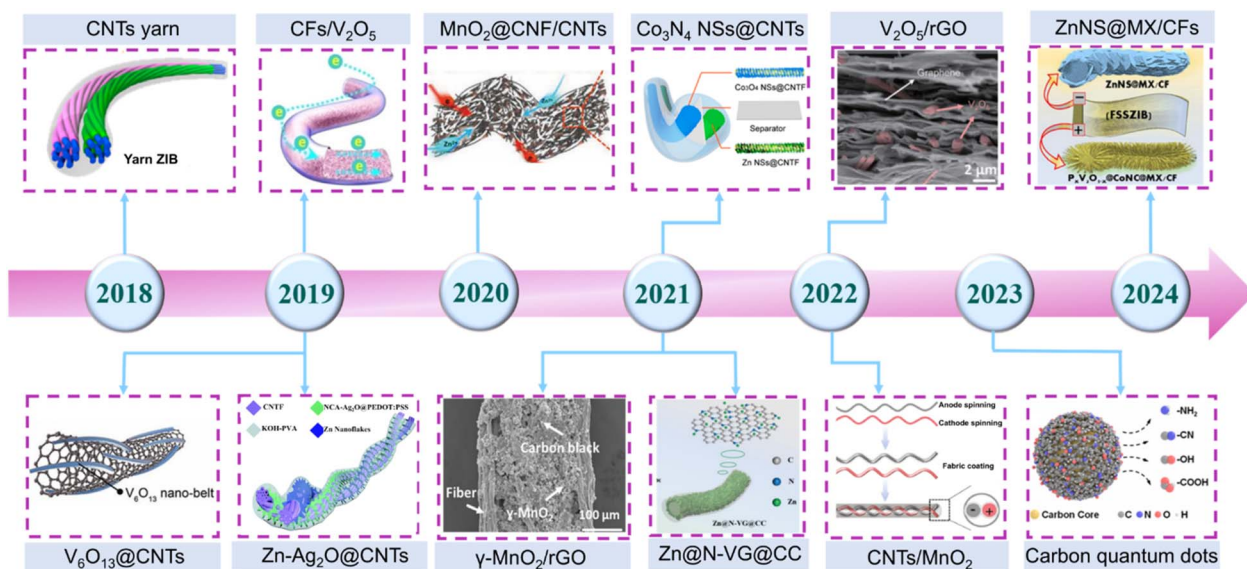


Fig. 2 Timeline of representative research work on the application of carbon nanomaterials in FZIBs. Reproduced from ref. 36 with permission from Wiley-VCH, copyright 2021. Reproduced with permission from ref. 37. Copyright 2022 Elsevier. Reproduced with permission from ref. 38. Copyright 2024 Elsevier. Reproduced from ref. 39 with permission from Wiley-VCH, copyright 2020. Copyright 2019 Royal Society of Chemistry. Reproduced with permission from ref. 40. Reproduced with permission from ref. 41. Copyright 2018 American Chemical Society. Reproduced with permission from ref. 42. Copyright 2021 Royal Society of Chemistry. Reproduced with permission from ref. 43. Copyright 2023 American Chemical Society. Reproduced with permission from ref. 44. Copyright 2021 American Chemical Society. Reproduced from ref. 45 with permission from Wiley-VCH, copyright 2022. Reproduced with permission from ref. 46. Copyright 2019 American Chemical Society. Reproduced from ref. 47 with permission from Wiley-VCH, copyright 2022.

oxide, *etc.*) undergoes a reduction reaction, resulting in the embedding of Zn<sup>2+</sup> within the cathode material. The charging process is the inverse of the aforementioned process, with Zn<sup>2+</sup> in the positive electrode material released and migrating back to the zinc anode (Fig. 3a).<sup>54</sup> The zinc anode undergoes a reduction reaction, resulting in the deposition of zinc metal while electrons flow back into the external circuit of the battery.<sup>55</sup> The long-term cycling stability of FZIBs in hydrogel electrolytes can be observed by the capacity retention after long-term cycling.<sup>56</sup> This process is dependent on a number of factors, including dendrite growth, corrosion, and the HER.<sup>57</sup> Furthermore, the cathode material is susceptible to volume changes and eventual dissolution in the electrolyte.<sup>58</sup> Carbon nanomaterials have unique advantages in solving these inherent problems. CNTs have excellent electrical conductivity and mechanical strength, rendering them suitable for use as a conductive substrate or 3D network for electrodes. This approach has been shown to enhance the efficiency of electron transfer and inhibit the dissolution of electrode materials. Currently, the production cost of CNTs is relatively high; however, with the advancement of production technology, a reduction in cost is anticipated. The application of CNTs in FZIBs can be extended to large-scale battery textiles, which has the potential for practical application in wearable electronic devices. Carbon fibers (CFs) are typically produced at a low cost, which is conducive to mass production. CFs possess good flexibility and conductivity, which can be used as reinforcements for electrode materials to improve the structural stability and electrochemical performance of batteries. The application

of CFs can facilitate the integration of FZIBs in flexible electronic devices, and improve the mechanical adaptability and durability of the devices. The preparation of CDs is typically inexpensive and the production of large quantities is straightforward. CDs have quantum-limited domain effects, exhibit tunable optical properties and good chemical stability, and provide additional functionality for batteries, such as fluorescent properties. The production cost of GO is dependent on the preparation method employed, but it is typically cost-effective. GO exhibits high chemical stability and a high specific surface area, which can be utilized as the primary framework of the cathode to enhance the cycling stability of batteries. The application of GO in FZIBs contributes to the improvement of charging and discharging rates and the overall performance of the batteries, particularly in smart textiles and self-powered systems. A thorough examination of the associated costs, functional capabilities and potential applications can offer guidance for subsequent research and facilitate the advancement and commercialization of FZIB technology. The practical application of FZIBs is determined by their interface stability, mechanical strength and electrochemical properties in the deformation state.<sup>59</sup>

## 2.2 Structural designs

As illustrated in Fig. 3b, FZIBs can be constructed in various structural configurations, including coaxial, twisting, parallel and crossing, which are one-dimensional (1D) structures that are more suitable for the fabrication of battery textiles.<sup>60</sup> In comparison to fiber-based batteries, two-dimensional (2D)





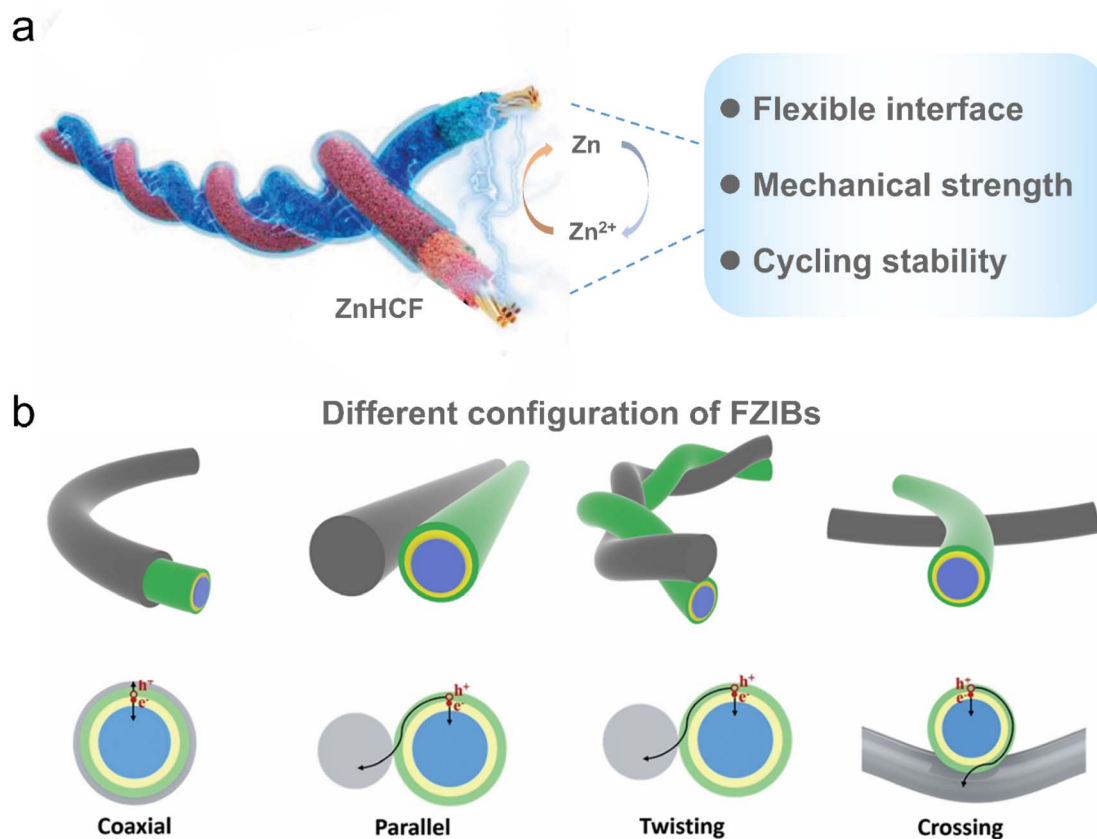


Fig. 3 (a) Schematic diagram of the energy storage mechanism of FZIBs, highlighting the key factors influencing their practical application. Reproduced from ref. 59 with permission from Elsevier, copyright 2024. (b) Different structural forms of FZIBs and their charge transfer pathways. Reproduced with permission from ref. 60. Copyright 2022 American Chemical Society.

flexible batteries are not well-suited for large-scale weaving and exhibit poor breathability in wearable devices.<sup>61</sup> In parallel structures, fiber electrodes are arranged in parallel, with an isolation layer typically placed between them to prevent short circuits.<sup>44</sup> FZIBs can be conveniently combined in series or parallel when configured in parallel.<sup>62</sup> In conventional textile technology, the process of twisting and integrating the electrodes is analogous to the twisting process in textiles. The twisting angle can be varied by precisely adjusting the relative position between the fiber electrodes, the rotation rate, and the translation speed. The twisted configuration of the electrodes can be achieved, which facilitates large-scale production. The twisted structure of FZIBs can be more easily woven into battery textiles at a certain scale due to its similar structure to textile yarns. The traversing structure exhibited a lack of interfacial contact when compared to the twisted structure, which demonstrated the ability to enhance interfacial contact to a certain extent by regulating the number of windings.

In these various configuration designs, coaxial structures offer shorter ion transport paths and greater stability during mechanical bending due to their higher interfacial area and great electrode contact.<sup>55</sup> Nevertheless, the precise assembly of an integrated cell is a challenging process. In light of these considerations, the twisted structure may be the optimal choice

for achieving satisfactory scalability, given its stable electrochemical performance and proper assembly feasibility.

### 3. Carbon nanomaterials for FZIBs cathodes

#### 3.1 Carbon nanomaterials as a conductive matrix

Both manganese-based<sup>63</sup> and vanadium-based oxide materials<sup>64</sup> have been extensively studied as cathode materials for ZIBs due to their typical long-range ordered crystal structures and layered framework characteristics. These characteristics provide space for reversible redox reactions of Zn<sup>2+</sup> insertion/extraction. Nevertheless, the geometric structure of the material undergoes volume changes during electrochemical processes, which results in slow kinetic reactions.<sup>65</sup> Amorphous materials include PBAs and organic materials,<sup>66</sup> but they usually demonstrate moderate capacity. In conclusion, the cathode materials are generally characterized by insufficient conductivity and inferior contact with the flexible interface under actual working conditions, which collectively result in low Zn<sup>2+</sup> transport efficiency and represent a significant impediment to the advancement of FZIB technology. To overcome these challenges, a cost-effective solution strategy involves combining active substances with carbonaceous conductive substrates. Carbon nanomaterials can be used as the main frame of the cathode,



providing enough space to accommodate volume expansion and contraction, thereby improving the cycle stability.<sup>67</sup> The excellent conductivity and high specific surface area permit a significant enhancement of the ion diffusion rate and charge/discharge rate of the electrodes.<sup>68–70</sup> Consequently, they are widely investigated in the optimization and innovative design of cathode materials. CNTs have the advantages of remarkable electrical conductivity, great flexibility and shape tunability.<sup>71–73</sup>

For example, CNTs were usually utilized as a conductive substrate to grow Co-based MOF arrays, which were then oxidized and etched *in situ* to obtain three-dimensional(3D)  $\text{Co}_3\text{O}_4$  nanosheet arrays, and the nanosheets were well distributed on the CNTs (Fig. 4a and c).<sup>44</sup> The CNTs imparted high flexibility and good conductivity to the cathode, resulting in stable resistance after the electrode was bent several times at different bending angles, indicating that the CNTs promoted

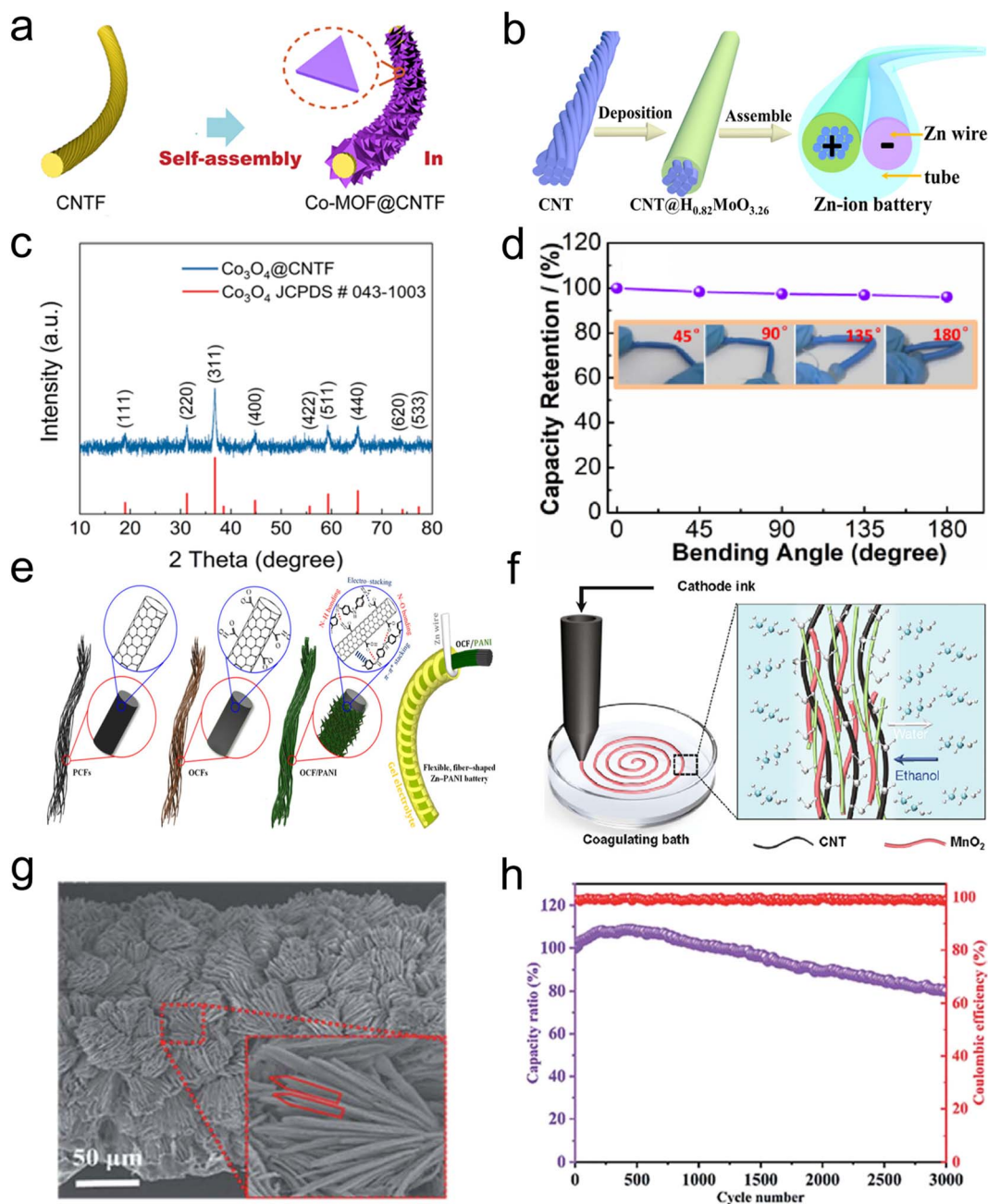


Fig. 4 (a) Schematic diagram of the preparation process of fiber-shaped  $\text{Co}_3\text{O}_4$ @CNT electrodes and (c) XRD pattern of the  $\text{Co}_3\text{O}_4$ @CNTs. Reproduced with permission from ref. 44. Copyright 2021 American Chemical Society. (b) Schematic illustration of the fiber-shaped Zn-ion battery and (d) the capacity retention at different bending angles. Reproduced with permission from ref. 77. Copyright 2022 Elsevier. (e) Schematic preparation of OCF/PANI electrode-based flexible FZIBs. Reproduced with permission from ref. 88. Copyright 2020 American Chemical Society. (f) Wet-spun fiber-shaped electrodes. Reproduced with permission from ref. 37. Copyright 2022 Elsevier. (g) SEM image of the  $\text{Mn}_2\text{O}_3$ @C/CNT electrode and (h) cycling performance of the FZIBs at 3 A  $\text{cm}^{-3}$ . Reproduced with permission from ref. 96. Copyright 2020 Royal Society of Chemistry.



the electrochemical stability of the flexible electrode structure. Amorphous materials are characterized by an open framework structure and the presence of sufficient active sites. However, their capacity and long-term cycle stability still need further improvement. Additionally, CNTs can be employed as the deposition sites of amorphous materials.<sup>74–76</sup> For amorphous  $\text{H}_{0.82}\text{MoO}_{3.26}$  (ref. 77) (Fig. 4b), protons ( $\text{H}^+$ ) and  $\text{Zn}^{2+}$  can be reversibly transported inside. Meanwhile they can also act as additional charge carriers during the charging and discharging process. The excellent structural stability, efficient charge transport and high mechanical toughness of CNTs enable the FZIBs, which consists of this cathode material and a zinc metal wire anode, to achieve an energy density of up to  $32.1 \text{ mW h cm}^{-3}$  based on the cathode volume at a current density of  $700 \text{ mA cm}^{-3}$ , while maintaining a high capacity of approximately 67% during charging and discharging. Furthermore, the battery demonstrates remarkable flexibility even after 5000 cycles, with a capacity retention rate of approximately 91% even after 3500 bending tests. The FZIB with CNTs as the cathode material also exhibits remarkable flexibility.<sup>78–80</sup> Following testing at various bending angles and durations (Fig. 4d), the battery demonstrated a capacity retention of up to 96% when bent from  $45^\circ$  to  $180^\circ$ . For composite materials comprising carbon nanomaterials in battery cathodes, the stability of the interface is of paramount importance in determining the electrochemical stability.<sup>81–85</sup> Inadequate interfacial bonding of composite electrode materials frequently results in limited capacity retention. The conventional approach to interfacial treatment for carbon nanomaterials is surface modification by acidification. Acid treatment can increase the hydrophilic functional groups on the carbon nanomaterials, thereby enhancing the interaction between the two phases of the composite material which improves the charge storage inside the electrode.<sup>86,87</sup> In addition, Yu *et al.*,<sup>88</sup> improved the electrochemical performance of polyaniline (PANI) by plasma-assisted surface modification of CFs (Fig. 4e). The specific surface area and pore volume of the plasma-treated CFs were found to be significantly increased. During the electrodeposition process, the aniline molecules reacted with the oxygen-containing groups on the surface of the CF to form N–O, N–H bonds and  $\pi$ – $\pi$  stacking structures, which helped to build a uniform and highly loaded PANI layer. The derived structure not only enhances the binding force between PANI and CFs, but also effectively inhibits PANI decomposition. Thanks to the excellent flexibility of the original CF, FZIBs maintain a high capacitance retention rate even after repeated bending.

Wet spinning technology is a mature process in fiber preparation and can be widely used in the production of fiber electrodes. This technology has significant advantages such as low cost, rapid preparation and scalability and is expected to bring FZIBs to large scale production.<sup>89–93</sup> Gao *et al.*<sup>37</sup> prepared spinning inks by mixing the synthetic manganese dioxide nanowire active material, cellulose nanofiber (CNF) solution and CNTs. The spinning inks were extruded and then transferred directly to a solvent-exchange bath, where they rapidly transformed into gel fibers. After the solvent was completely evaporated, the fibers formed the fibrous electrodes as shown in Fig. 4f.

### 3.2 Carbon nanomaterials as encapsulation layers

Most cathode host materials have poor electrode stability and rapid dissolution due to their high surface energy.<sup>94</sup> The introduction of a carbon-based encapsulation material onto the electrode surface has been shown to be an effective strategy to inhibit these problems by acting as an electrode protective layer to isolate direct contact with the electrolyte.<sup>95</sup> In addition, carbon-based encapsulants can also promote rapid electron transfer and improve electrochemical performance. Liu *et al.*<sup>96</sup> vertically grew 3D  $\text{Mn}_2\text{O}_3$ @C flakes on CNTs by a simple hydrothermal method (Fig. 4g), with organic ligands carbonized *in situ* to form a coating layer. The vertically stacked structure increases the contact area between the cathode and the electrolyte, creating stable ionic transport. Simultaneously, it can be used as a packaging layer to reduce damage to the material structure caused by volume changes. The carbon layer could prevent the active material from coming into direct contact with the electrolyte, thereby inhibiting side reactions. This protection results in a high-capacity retention rate even after a long-term cycle, as shown in Fig. 4h. In addition, wet spinning technology represents an effective means of preparing fibrous electrodes. The uniformity of the spinning solution represents an important factor affecting the spinning results. Xia *et al.*<sup>47</sup> introduced GO to improve the rheological behavior of  $\text{V}_2\text{O}_5$  nanowire dispersions, regulating the rheological and liquid crystal behavior of the dispersion. The introduction of GO sheets enhanced the electrostatic interactions and entropy-driven volume exclusion effects between  $\text{V}_2\text{O}_5$  nanowires, promoting the directional alignment of  $\text{V}_2\text{O}_5$  nanowires. The intimate contact between GO sheets and  $\text{V}_2\text{O}_5$  nanowires serves to reinforce the structural integrity, mechanical strength and electrical conductivity of the derived hybrid fiber. This enables the battery to maintain its structural integrity during the charging and discharging processes, while also improving the flexibility and long-term electrochemical stability of the fibrous electrode.

## 4. Carbon nanomaterials for FZIBs anodes

### 4.1 Carbon nanomaterials as current collectors

Conventional aqueous ZIBs predominantly utilize zinc foil as the anode, which constrains the applicability of the battery in the field of flexible energy storage devices.<sup>51</sup> In contrast, FZIBs typically employ zinc wire, zinc coated fiber or zinc powder derived fiber as the anode.<sup>97</sup> Zinc powder-based anodes are potential candidates for commercial applications due to their high scalability and adjustable loading capacity.<sup>98–100</sup> However, the 3D spherical structure of zinc powder gives it higher reactivity, which can further exacerbate electrochemical corrosion and side reactions, especially at the interface between the electrode and the electrolyte.<sup>27,101</sup> The uniform deposition of  $\text{Zn}^{2+}$  has been demonstrated to be an effective means of alleviating the aforementioned issues.<sup>102–104</sup> Concurrently, numerous researchers have posited that the optimal approach to uniform  $\text{Zn}^{2+}$  deposition and the





prevention of dendrite growth is the design of zinc anodes with a high specific surface area and high conductivity.<sup>105</sup> Carbon-based substrates, such as carbon cloth (CC) and CNTs, offer a number of advantages over flat zinc foil.<sup>106</sup> Firstly, they provide more accessible active sites for zinc deposition, which is beneficial for uniform deposition. Secondly, they help to control dendrite growth and accommodate volume changes, which is important for preventing dendrite growth and ensuring the stability of the battery. The flexibility of these materials far exceeds that of zinc foil, rendering them applicable in FZIBs in a wide range of contexts. It is clear that carbon nanomaterials, with their light weight and excellent

electrical conductivity,<sup>107</sup> are important current collectors for improving the reaction kinetics.<sup>108–110</sup> A number of recent studies have investigated a range of carbon-based modification strategies for stabilizing zinc anodes.

Cong *et al.*<sup>111</sup> employed the electrodeposition method to deposit zinc on CFs. The porous structure of the CFs facilitated the uniform deposition of  $\text{Zn}^{2+}$  on the electrode surface, thereby reducing the overpotential. This resulted in the formation of a channel for the rapid diffusion of  $\text{Zn}^{2+}$ , which reduces the ion transport resistance. Ultimately, this inhibited the growth of zinc dendrites (Fig. 5a) while improving the cycle stability and safety of the battery. The hybrid electrode exhibited enhanced

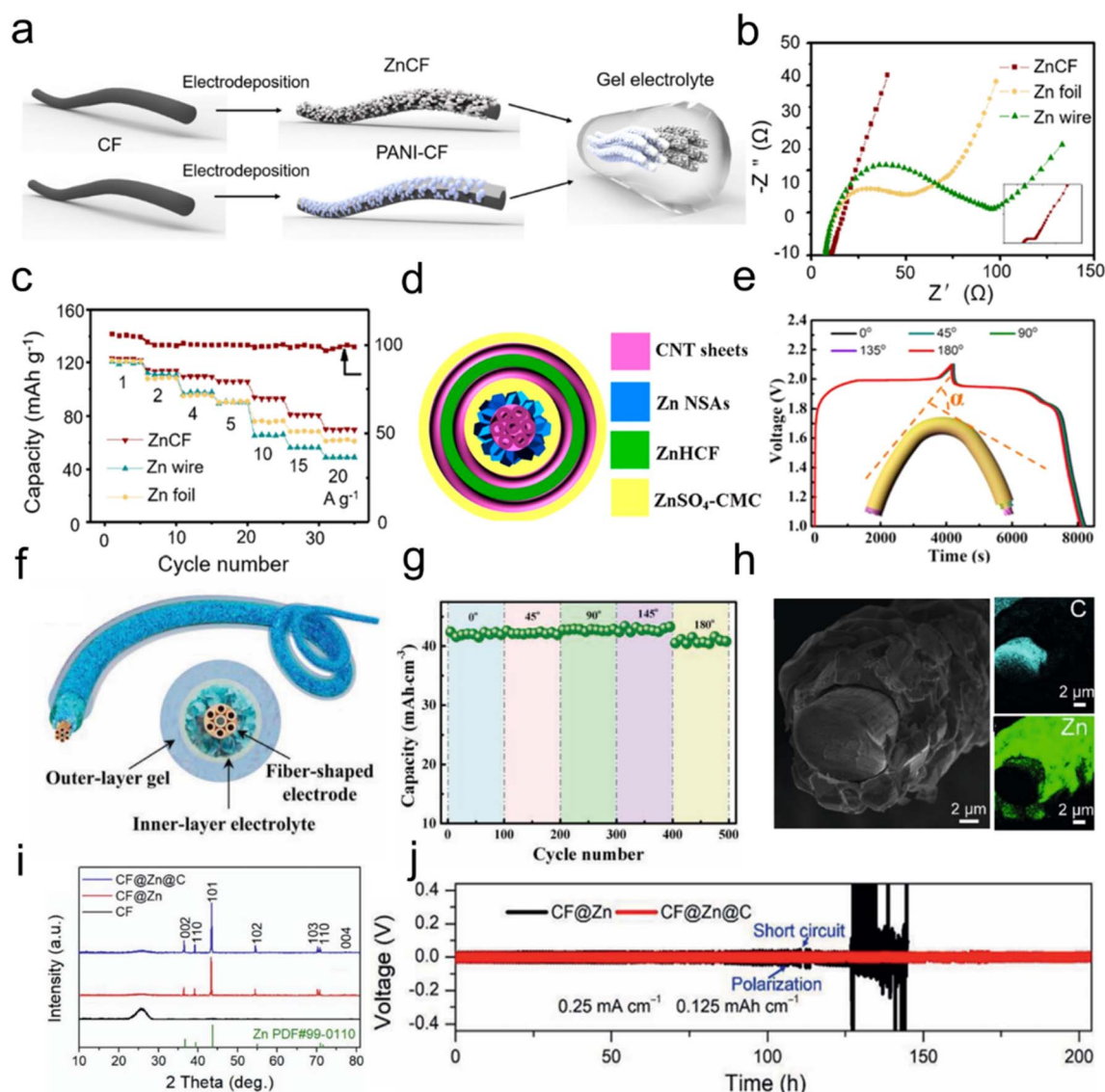


Fig. 5 (a) Schematic illustration of the fabrication of a solid-state fiber-shaped Zn/PANI battery, (b) rate performance of batteries at different current densities, and (c) Nyquist plots of the batteries. Reproduced with permission from ref. 111. Copyright 2021 American Chemical Society. (d) Schematic illustration of the cross-section view of the batteries and (e) charge–discharge curves of the batteries at a current density of  $0.1 \text{ A cm}^{-2}$  at different bending angles. Reproduced with permission from ref. 112. Copyright 2019 American Chemical Society. (f) The schematic illustration of Zn@CNTs and (g) the capacity of FZIBs versus bending angles. Reproduced from ref. 59 with permission from Wiley-VCH, copyright 2024. (h) Cross-sectional SEM image of CF@Zn, (i) XRD patterns of CF, CF@Zn, and CF@Zn@C, and (j) voltage–time profiles of the symmetric cells. Reproduced from ref. 119 with permission from Wiley-VCH, copyright 2021.



stability in the deposition and stripping processes, accompanied by a reduction in polarization (30 mV) in comparison to Zn foil and Zn wire electrodes. This was evidenced by a higher capacity retention and a smaller charge transfer resistance (Fig. 5b and c). This is contingent upon the electrode surface exhibiting high conductivity and a high surface area. Furthermore, CNTs have a multitude of applications in zinc anodes due to their high mechanical strength and flexibility, which can be combined with a variety of device structures. The interface between the zinc anode and electrolyte is a crucial area where electrochemical reactions occur. Zinc dendrite growth and side reactions occur at the interface, and the stability of this interface has a significant impact on battery performance. The coaxial structure has a larger area of interface contact than the traditional parallel structure,<sup>112</sup> so the coaxial structure is one of the ideal structural designs for FZIBs. Zhang *et al.* employed CNTs as the host material for the coaxial device, conferring long-term mechanical flexibility and stability (Fig. 5d) while maintaining a stable electrochemical interface following repeated bending at large angles (Fig. 5e). Following 3000 cycles of 90° bending, the capacity retention rate exceeded 90%. CNTs exhibit considerably higher conductivity than traditional electrode materials. They can facilitate the formation of additional electron transport channels, thereby enhancing the conductivity of the electrode. Furthermore, they can facilitate the electron transport rate during the charging and discharging process. CNTs can be employed as a support for active materials such as zinc and zinc hexacyanoferrate (ZnHCF), thereby providing a greater number of active sites (Fig. 5f). This increases the contact area between the electrode and the electrolyte, which in turn enhances the capacity and power density.<sup>59</sup> The intimate contact between the CNTs and the gel electrolyte ensures the maintenance of a secure bond between the electrode and the electrolyte, even when the battery is subjected to deformation (Fig. 5g). This is of particular significance for flexible batteries.

#### 4.2 Carbon nanomaterials as protecting layers

To prevent the risk of short circuits caused by dendrites growing through the separators, it is more straightforward to build a protective layer. Recent studies have demonstrated the efficacy of constructing artificial interface protective layers on zinc anodes as a strategy for regulating the electric field to alleviate zinc corrosion.<sup>113–115</sup> In this context, carbon nanomaterials have emerged as a crucial material for electrode modification in flexible energy storage devices, due to their high specific surface area and stability.<sup>116–118</sup> Zhai *et al.* employed magnetron sputtering to uniformly prepare a carbon nanocoating on the zinc anode (Fig. 5h and i). The carbon layer functions as an electron conductor, which can facilitate a more uniform electric field distribution on the zinc anode surface, thereby enhancing the smoothness of the zinc deposition process.<sup>119</sup> At the interface of the stripping reaction, the conductive carbon layer can optimize the electron distribution, and reduce preferential dissolution. The graphite nature of the carbon layer endows it with good ductility and compressibility, thereby providing additional soft

surfaces and abundant nucleation sites. These characteristics facilitate uniform zinc deposition and the reduction of grain size. The CFs@Zn-based symmetric cell exhibited significant voltage fluctuations after approximately 100 hours, indicative of the formation and growth of zinc dendrites, which ultimately resulted in a short circuit within the cell. In contrast, the CFs@Zn@C-based symmetric cell exhibited a stable voltage curve even after 200 hours (Fig. 5j), indicating superior deposition/stripping stability. The carbon layer also serves to enhance the stability and water resistance of the cell under extreme deformation conditions, thereby expanding the potential applications of FZIBs to a wide range of wearable electronics.<sup>120,121</sup> These studies have demonstrated the significant value of carbon nanomaterials in improving the performance.

## 5. Carbon nanomaterials for FZIBs electrolyte

The quasi-solid gel electrolyte represents the principal form of electrolyte employed in FZIBs. Currently, issues such as low ionic conductivity and insufficient mechanical strength are prevalent, influencing the charging and discharging rate and overall performance of the battery.<sup>122,123</sup> The stretching or bending behavior during actual wearable processes can result in poor contact between the electrolyte and the electrode, which is not conducive to the stability and cycle life of the battery.<sup>124–127</sup> The incorporation of additives into the electrolyte can facilitate the even distribution of ions at the interface, while simultaneously inhibiting the occurrence of side reactions and achieving uniform zinc deposition.<sup>128,129</sup> Xiao *et al.*<sup>130</sup> introduced GO as an additive to the polyvinyl alcohol (PVA) gel electrolyte (Fig. 6a). GO exhibits high ionic conductivity and a large specific surface area, which facilitates the transport of ions within the electrolyte. GO sheets are uniformly dispersed in the gel electrolyte, forming a continuous, interconnected ion transport path (Fig. 6b). The appropriate quantity of GO flakes can prevent stacking and maintain the ion transport path in an unobstructed state. The hydrogen bonding between GO and the PVA matrix enhances the mechanical strength of the gel electrolyte, which enables it to maintain a tight assembly under large deformation (Fig. 6c). This ensures reliability and safety of use, maintaining the structure integrity.

Zero-dimensional (0D) carbon nanomaterials manifest plenty of distinctive advantages. One is the small size of 0D CDs, included quantum confinement effects, which can alter the electronic structure and optical properties of CDs.<sup>131–134</sup> This enables them to exhibit tunable fluorescence emission wavelengths and absorption characteristics. Furthermore, CDs are chemically stable, which is beneficial for retaining their structure and functionality in a range of chemical environments.<sup>135</sup> Liu *et al.* employed zinc wires as anodes and self-supported PBAs as cathodes, and introduced a fluorescent carbon dot-modified gel electrolyte between the two to successfully assemble a fluorescent fiber water-based zinc ion battery for high-voltage platforms.<sup>43</sup> The uneven electric field and





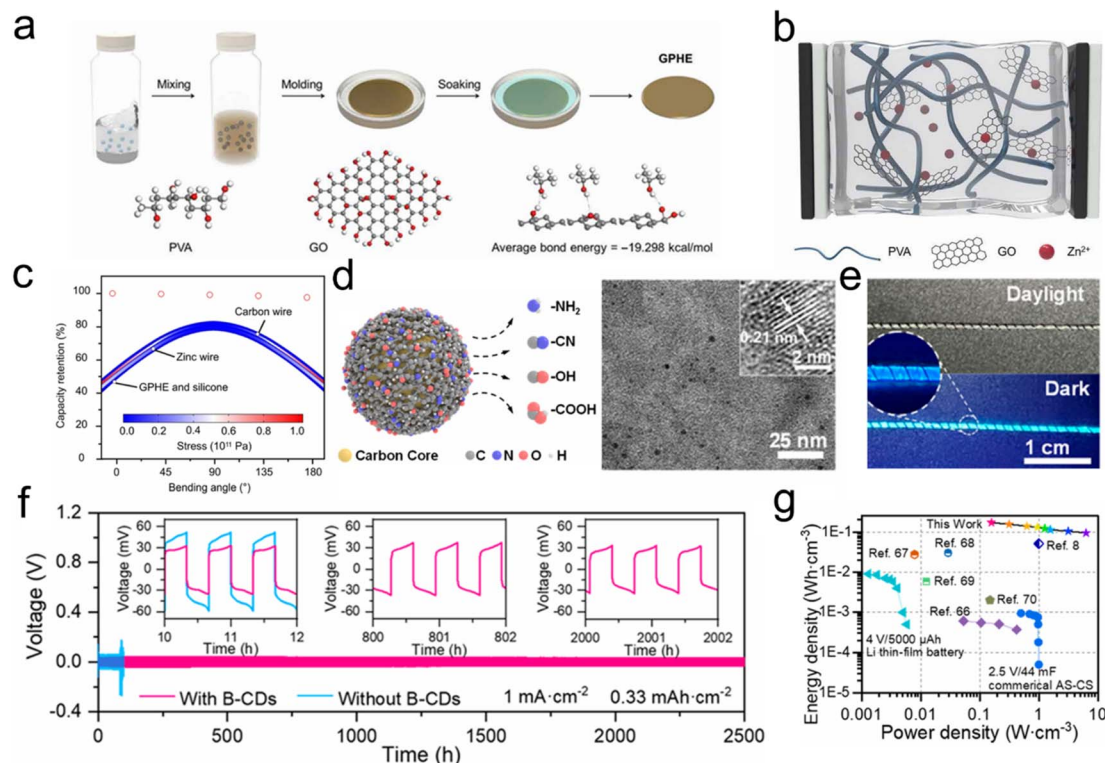


**Fig. 6** (a) Schematic diagram of the preparation process of hydrogel electrolytes, (b) schematic diagram of the ion-conducting process of hydrogel electrolytes and (c) bending stress and deformation of a 3 cm ZIB fiber. Reproduced with permission from ref. 130. Copyright 2021 American Association for the Advancement of Science. (d) Schematic illustration of B-CDs and TEM image of B-CDs and (e) FZIBs under daylight and in a dark environment with 365 nm excitation. (f) Cycling performance of the symmetric cells and (g) the device was compared with the recently reported battery. Reproduced with permission from ref. 43. Copyright 2023 American Chemical Society.

inevitable corrosion of the zinc wire itself resulted in the observed dendritic growth of the zinc anode with limited cycle reversibility. The CDs, with their numerous zinc-binding sites (Fig. 6d), can form an ultrathin  $\text{Zn}^{2+}$  adsorption layer on the metal zinc surface, thereby optimizing the electric field distribution and reducing the nucleation energy potential. This results in stable and reversible plating/stripping of zinc within 2500 h. FZIBs tend to deliver a high power output while maintaining high energy density (Fig. 6f and g). The average diameter of the CDs is 2.3 nm. The high-resolution transmission electron microscopy (HRTEM) image shows a lattice spacing of 0.21 nm, indicating a high degree of crystallinity (Fig. 6e). A multicolored textile was created by weaving fluorescent fibers with different luminescent properties into a wearable battery display system, thus achieving lightweight and multifunctional flexible fabrics.

## 6. Applications in an integrated system

Currently, the development of smart textiles driven by FZIBs is underway, with the eventual goal of integrating these technologies into the fabric of daily life.<sup>136–139</sup> The incorporation of FZIBs into smart textiles is intended to increase the comfort of future social interactions. FZIBs can be integrated with existing sustainable energy harvesting systems and sensors. For instance, Xia *et al.*<sup>47</sup> proposed an integrated energy solution

with the objective of developing wearable electronic devices and portable energy systems. The researchers combined FZIBs with high-efficiency GaAs solar cells to create a self-powered system that can collect solar energy during the day and store it in the fiber cells (Fig. 7b). This system can then supply power to electronics when needed, achieving smart textiles with both energy harvesting and storage capabilities. As a sustainable and stable power source, it can also be used to drive a network of human sensors for personalized healthcare (Fig. 7a). Zhang *et al.*<sup>140</sup> developed a light-powered textile using an industrial shuttle-flying weaving process, which comprises a photovoltaic energy-harvesting module and a rechargeable textile battery. Furthermore, the device is capable of functioning in a twisted and wet environment, and can store energy for over 60 days without significant voltage loss. In energy utilizing systems, FZIBs can be integrated with fiber strain sensors to monitor the movement of different parts of the human body, including the elbows, fingers, wrists, and knees (Fig. 7c). The multifunctional battery with an integrated strain sensor offers new avenues for future wearable electronics, particularly in the domains of health monitoring, electronic skin, and human–computer interaction.<sup>141</sup> As a portable energy module, it can provide a stable power supply in extreme environments,<sup>142</sup> for example, washing, beating and burning (Fig. 7d). Xiao *et al.* integrated a textile battery with electronic sensors and a wireless charging terminal into a knitted shirt to construct a wireless charging



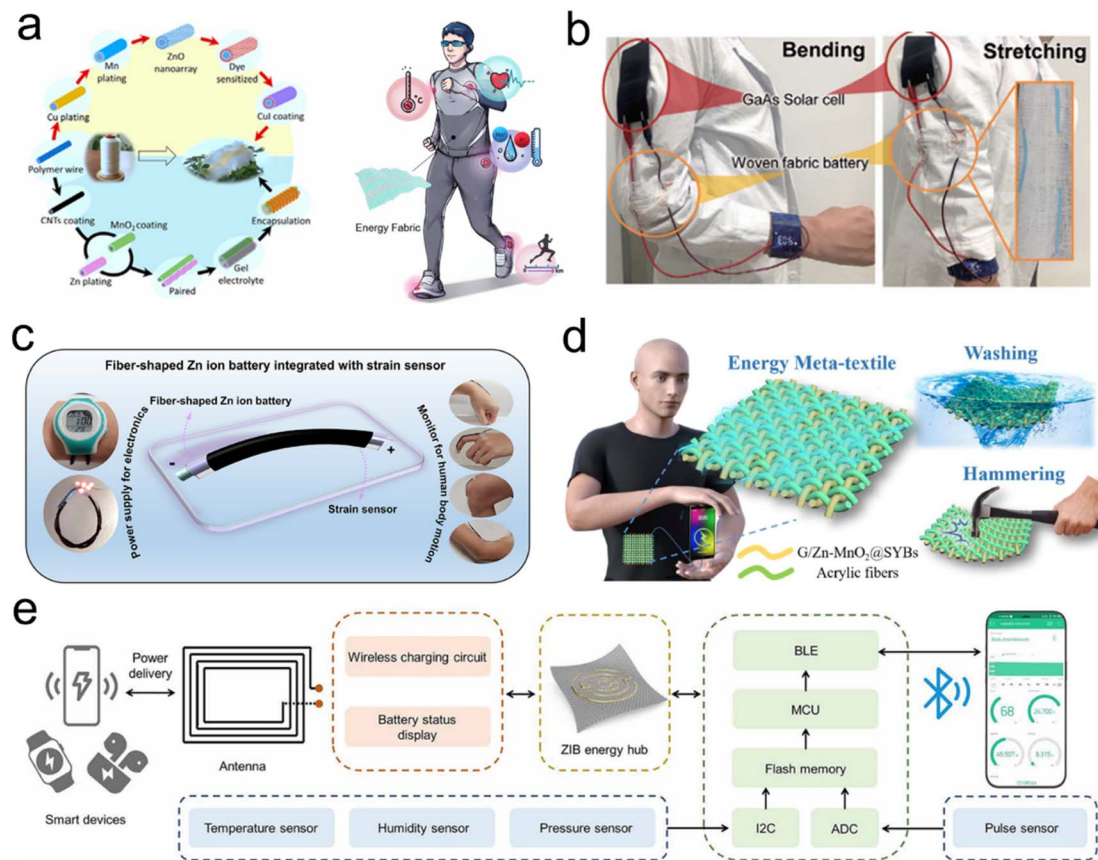


Fig. 7 (a) The process of manufacturing functional fibers and the application of human body area sensor networks. Reproduced with permission from ref. 140. Copyright 2020 Elsevier. (b) A self-powered integrated system for wearable devices. Reproduced with permission from ref. 47 with permission from Wiley-VCH, copyright 2022. (c) FZIBs integrated with strain sensors. Reproduced with permission from ref. 141. Copyright 2022 American Chemical Society. (d) Schematic diagram of the battery textile. Reproduced with permission from ref. 142. Copyright 2024 Elsevier. (e) FZIB powered textile body area network wearable system block diagram. Reproduced with permission from ref. 130. Copyright 2021 American Association for the Advancement of Science.

and sensing system. This textile-based body area network (Fig. 7e) can be used as a power unit on the body to monitor the heart rate, temperature, humidity and altitude.<sup>130</sup>

## 7. Conclusions and perspective

To further meet the demands of wearable electronics, the development of FZIBs with excellent mechanical adaptability, durability and high capacity is the future research direction. This review summarizes the application of carbon nanomaterials in the cathode, anode and device configuration of FZIBs. The incorporation of carbon nanomaterials into the cathode, anode and device structure of FZIBs significantly enhances the cycle stability and energy density. As a fibrous conductive skeleton, they permit the fibers to be woven into flexible battery components, thereby conferring good mechanical and electrochemical properties. Carbon-based fiber electrodes can be combined with a polymer matrix to form composite fibers that exhibit both high conductivity and resilience to mechanical stress. Nevertheless, numerous obstacles remain that impede the further commercialization of these materials.

(1) Design and preparation of carbon-based composite electrodes. The preparation of fibrous electrodes necessitates consideration of both flexibility and electrochemical properties. Currently, the preparation of carbon-based composite electrodes employs a variety of techniques, including simple hydrothermal methods, high-temperature carbonization, wet spinning and electrodeposition. However, the challenge remains in achieving an optimal balance between the synergistic effects of active materials and carbon nanomaterials.

(2) Flexible mechano-electrochemical properties of FZIBs are extremely critical. FZIBs necessitate a stable energy supply under long-term mechanical deformation, yet frequently encounter electrochemical performance deterioration during cycling. The elucidation of the original mechanism and structure-activity relationship of carbon nanomaterials in the flexible mechano-electrochemical properties is of great significance for the design of flexible electrodes.

(3) Integrated application of continuous scale preparation technology in FZIBs, including integrated forming spinning, scale-up spinning slurry preparation, and continuous assembly of fiber cells. FZIBs have a multitude of potential applications in biosensors, artificial intelligence, and medical equipment.



Furthermore, there is currently no uniform testing and production standard for evaluating the functionality of wearable smart textiles.

## Data availability

All consent forms have been duplicated from the publisher with the necessary permissions to publish the data.

## Author contributions

Guoqing Lu: conceptualization, data curation, writing – original draft. Qiqing Xi: data curation, writing – review & editing. Yanyan Shao: resources, data curation. Yinan Yang: writing – review & editing. Yichuan Rui: supervision, writing – review & editing. Yuanlong Shao: resources, writing – review & editing.

## Conflicts of interest

There are no conflicts to declare.

## Acknowledgements

This work was financially supported by the National Natural Science Foundation of China No. T2188101, Gusu's young leading talent (ZXL2021449), and Key industry technology innovation project of Suzhou (SYG202108).

## References

- 1 R. Lin, H.-J. Kim, S. Achavananthadith, S. A. Kurt, S. C. C. Tan, H. Yao, B. C. K. Tee, J. K. W. Lee and J. S. Ho, *Nat. Commun.*, 2020, **11**(1), 444.
- 2 X. Zhao, Y. Zhou, J. Xu, G. Chen, Y. Fang, T. Tat, X. Xiao, Y. Song, S. Li and J. Chen, *Nat. Commun.*, 2021, **12**(1), 6755.
- 3 Y. Niu, H. Liu, R. He, Z. Li, H. Ren, B. Gao, H. Guo, G. M. Genin and F. Xu, *Mater. Today*, 2020, **41**, 219–242.
- 4 N. A. Choudhry, L. Arnold, A. Rasheed, I. A. Khan and L. Wang, *Adv. Eng. Mater.*, 2021, **23**(12), 2100469.
- 5 B. Zhang, X. Cai, J. Li, H. Zhang, D. Li, H. Ge, S. Liang, B. Lu, J. Zhao and J. Zhou, *Energy Environ. Sci.*, 2024, **17**, 3878–3887.
- 6 F. Mo, G. Liang, Z. Huang, H. Li, D. Wang and C. Zhi, *Adv. Mater.*, 2020, **32**(5), 1902151.
- 7 W. Wang, C. Li, S. Liu, J. Zhang, D. Zhang, J. Du, Q. Zhang and Y. Yao, *Adv. Energy Mater.*, 2023, **13**(18), 2300250.
- 8 X. Xu, S. Xie, Y. Zhang and H. Peng, *Angew. Chem., Int. Ed.*, 2019, **58**(39), 13643–13653.
- 9 H. Li, L. Ma, C. Han, Z. Wang, Z. Liu, Z. Tang and C. Zhi, *Nano Energy*, 2019, **62**, 550–587.
- 10 X. Zeng, J. Hao, Z. Wang, J. Mao and Z. Guo, *Energy Storage Mater.*, 2019, **20**, 410–437.
- 11 S. Lei, Z. Liu, C. Liu, J. Li, B. Lu, S. Liang and J. Zhou, *Energy Environ. Sci.*, 2022, **15**, 4911–4927.
- 12 S. Liu, L. Kang, J. M. Kim, Y. T. Chun, J. Zhang and S. C. Jun, *Adv. Energy Mater.*, 2020, **10**, 2000477.
- 13 Y. Liang, H. Dong, D. Aurbach and Y. Yao, *Nat. Energy*, 2020, **5**(9), 646–656.
- 14 T. Deng, L. Cao, X. He, A.-M. Li, D. Li, J. Xu, S. Liu, P. Bai, T. Jin, L. Ma, M. A. Schroeder, X. Fan and C. Wang, *Chem*, 2021, **7**(11), 3052–3068.
- 15 J. Parker, C. Chervin, I. Pala, M. Machler, M. Burz, J. Long and D. Rolison, *Science*, 2017, **356**, 415–418.
- 16 Y. Dai, C. Zhang, J. Li, X. Gao, P. Hu, C. Ye, H. He, J. Zhu, W. Zhang, R. Chen, W. Zong, F. Guo, I. P. Parkin, D. J. L. Brett, P. R. Shearing, L. Mai and G. He, *Adv. Mater.*, 2024, **36**, 2310465.
- 17 J. Luan, H. Yuan, J. Liu and C. Zhong, *Energy Storage Mater.*, 2024, **66**, 103206.
- 18 Y. Bai, Y. Qin, J. Hao, H. Zhang and C. M. Li, *Adv. Funct. Mater.*, 2023, **34**, 2310393.
- 19 Q. Liu, Z. Ma, Z. Chen, M. Cui, H. Lei, J. Wang, J. Fei, N. He, Y. Liu, Q. Liu, W. Li and Y. Huang, *Chem. Commun.*, 2022, **58**, 8226–8229.
- 20 Z. Wang, X. Zhu, X. Tao, P. Feng, J. Wang and J. Chen, *Adv. Funct. Mater.*, 2024, **34**, 2316223.
- 21 L. Zhou, W. Zhou, H. Wang, Q. Deng, X. Ai, X.-X. Zeng, X. Wu, C. Zhou and W. Ling, *Chem. Eng. J.*, 2024, **492**, 152324.
- 22 J. Zhang, M. Shi, H. Gao, X. Ren, J. Cao, G. Li, A. Wang and C. Liu, *Chem. Eng. J.*, 2024, **491**, 152050.
- 23 T. Zhou, L. Zhu, L. Xie, Q. Han, X. Yang, L. Chen, G. Wang and X. Cao, *J. Colloid Interface Sci.*, 2022, **605**, 828–850.
- 24 Y. He, Y. Pu, Y. Zheng, B. Zhu, P. Guo, X. Zhang, L. He, X. Wan and H. Tang, *J. Phys. Chem. Solids*, 2024, **184**, 111669.
- 25 L. Wu and Y. Dong, *Energy Storage Mater.*, 2021, **41**, 715–737.
- 26 B. K. Cho, S. H. Huh, S. H. Kim, S. Yu, J. S. Bae, J. K. Yoo and S. H. Yu, *Carbon Energy*, 2024, **6**, e441.
- 27 L. Zeng, J. He, C. Yang, D. Luo, H. Yu, H. He and C. Zhang, *Energy Storage Mater.*, 2023, **54**, 469–477.
- 28 X. Gao, C. Zhang, Y. Dai, S. Zhao, X. Hu, F. Zhao, W. Zhang, R. Chen, W. Zong, Z. Du, H. Dong, Y. Liu, H. He, J. Li, I. P. Parkin, G. He and C. J. Carmalt, *Small Struct.*, 2023, **4**, 2200316.
- 29 H. Ying, P. Huang, Z. Zhang, S. Zhang, Q. Han, Z. Zhang, J. Wang and W.-Q. Han, *Nano-Micro Lett.*, 2022, **14**, 180.
- 30 W. Fan, J. Wu and H. Wang, *Mater. Res. Lett.*, 2023, **11**, 481–516.
- 31 J. Wang, Y. Yang, Y. Zhang, Y. Li, R. Sun, Z. Wang and H. Wang, *Energy Storage Mater.*, 2021, **35**, 19–46.
- 32 Y. Gong and Y. Xue, *New Carbon Mater.*, 2023, **38**, 438–454.
- 33 X. Yu, Y. Fu, X. Cai, H. Kafafy, H. Wu, M. Peng, S. Hou, Z. Lv, S. Ye and D. Zou, *Nano Energy*, 2013, **2**, 1242–1248.
- 34 T. Xin, Y. Wang, Q. Xu, J. Shang, X. Yuan, W. Song and J. Liu, *ACS Appl. Energy Mater.*, 2022, **5**, 2290–2299.
- 35 H. Zhang, R. Guo, S. Li, C. Liu, H. Li, G. Zou, J. Hu, H. Hou and X. Ji, *Nano Energy*, 2022, **92**, 106752.
- 36 Q. Cao, H. Gao, Y. Gao, J. Yang, C. Li, J. Pu, J. Du, J. Yang, D. Cai, Z. Pan, C. Guan and W. Huang, *Adv. Funct. Mater.*, 2021, **31**, 2103922.





- 37 T. Gao, G. Yan, X. Yang, Q. Yan, Y. Tian, J. Song, F. Li, X. Wang, J. Yu, Y. Li and S. Guo, *J. Energy Chem.*, 2022, **71**, 192–200.
- 38 D. D. Khumujam, T. Kshetri, T. I. Singh, S. B. Singh, N. H. Kim and J. H. Lee, *Chem. Eng. J.*, 2024, **486**, 150252.
- 39 S. H. Kim, J. M. Kim, D. B. Ahn and S. Y. Lee, *Small*, 2020, **16**, 2002837.
- 40 C. Li, Q. Zhang, S. E. T. Li, Z. Zhu, B. He, Z. Zhou, P. Man, Q. Li and Y. Yao, *J. Mater. Chem. A*, 2019, **7**, 2034–2040.
- 41 H. Li, Z. Liu, G. Liang, Y. Huang, Y. Huang, M. Zhu, Z. Pei, Q. Xue, Z. Tang, Y. Wang, B. Li and C. Zhi, *ACS Nano*, 2018, **12**, 3140–3148.
- 42 M. Liao, J. Wang, L. Ye, H. Sun, P. Li, C. Wang, C. Tang, X. Cheng, B. Wang and H. Peng, *J. Mater. Chem. A*, 2021, **9**, 6811–6818.
- 43 F. Liu, S. Xu, W. Gong, K. Zhao, Z. Wang, J. Luo, C. Li, Y. Sun, P. Xue, C. Wang, L. Wei, Q. Li and Q. Zhang, *ACS Nano*, 2023, **17**, 18494–18506.
- 44 Y. Lu, H. Zhang, H. Liu, Z. Nie, F. Xu, Y. Zhao, J. Zhu and W. Huang, *Nano Lett.*, 2021, **21**, 9651–9660.
- 45 N. Subjalearndee, N. He, H. Cheng, P. Tesatchabut, P. Eiamlamai, P. Limthongkul, V. Intasanta, W. Gao and X. Zhang, *Adv. Fiber Mater.*, 2022, **4**, 457–474.
- 46 H. Wang, S. Zhang and C. Deng, *ACS Appl. Mater. Interfaces*, 2019, **11**, 35796–35808.
- 47 Z. Xia, S. Li, G. Wu, Y. Shao, D. Yang, J. Luo, Z. Jiao, J. Sun and Y. Shao, *Adv. Mater.*, 2022, **34**, 2203905.
- 48 Y. Li, Y. Guo, Z. Li, P. Wang, Y. Xie and T. Yi, *Energy Storage Mater.*, 2024, **67**, 103300.
- 49 C. Mao, Y. Chang, X. Zhao, X. Dong, Y. Geng, N. Zhang, L. Dai, X. Wu, L. Wang and Z. He, *J. Energy Chem.*, 2022, **75**, 135–153.
- 50 M. Xue, J. Bai, M. Wu, Q. He, Q. Zhang and L. Chen, *Energy Storage Mater.*, 2023, **62**, 102940.
- 51 Q. Li, N. Li and C. Zhi, *Nano Lett.*, 2024, **24**, 4055–4063.
- 52 Q. Wen, H. Fu, R. Cui, H. Chen, R. Ji, L. Tang, C. Yan, J. Mao, K. Dai, X. Zhang and J. Zheng, *J. Energy Chem.*, 2023, **83**, 287–303.
- 53 J. Yang, R. Zhao, Y. Wang, Z. Hu, Y. Wang, A. Zhang, C. Wu and Y. Bai, *Adv. Funct. Mater.*, 2023, **33**, 2213510.
- 54 F. Xiankai, X. Kaixiong, Z. Wei, D. Weina, Z. Hai, C. Liang and C. Han, *Carbon Energy*, 2024, e536.
- 55 L. Li, Y. Chen, S. Wang, D. Pei, M. Li, T. Li and C. Li, *Nano Energy*, 2024, **126**, 109662.
- 56 T. Zhang, Y. Tang, S. Guo, X. Cao, A. Pan, G. Fang, J. Zhou and S. Liang, *Energy Environ. Sci.*, 2020, **13**, 4625–4665.
- 57 X. Guo and G. He, *J. Mater. Chem. A*, 2023, **11**, 11987–12001.
- 58 Q. Xu, J. Chen, J. R. Loh, H. Zhong, K. Zhang, J. Xue and W. S. V. Lee, *Adv. Energy Mater.*, 2023, **14**, 2302536.
- 59 C. Li, W. Wang, J. Luo, W. Zhuang, J. Zhou, S. Liu, L. Lin, W. Gong, G. Hong, Z. Shao, J. Du, Q. Zhang and Y. Yao, *Adv. Mater.*, 2024, **36**, 2313772.
- 60 C. Chen, J. Feng, J. Li, Y. Guo, X. Shi and H. Peng, *Chem. Rev.*, 2022, **123**, 613–662.
- 61 Y. Liu, X. Zhou, Y. Bai, R. Liu, X. Li, H. Xiao, Y. Wang, X. Wang, Y. Ma and G. Yuan, *Chem. Eng. J.*, 2021, **417**, 127955.
- 62 M. Liao, C. Wang, Y. Hong, Y. Zhang, X. Cheng, H. Sun, X. Huang, L. Ye, J. Wu, X. Shi, X. Kang, X. Zhou, J. Wang, P. Li, X. Sun, P. Chen, B. Wang, Y. Wang, Y. Xia, Y. Cheng and H. Peng, *Nat. Nanotechnol.*, 2022, **17**, 372–377.
- 63 B. Wu, G. Zhang, M. Yan, T. Xiong, P. He, L. He, X. Xu and L. Mai, *Small*, 2018, **14**(13), 1703850.
- 64 M. Yan, P. He, Y. Chen, S. Wang, Q. Wei, K. Zhao, X. Xu, Q. An, Y. Shuang and Y. Shao, *Adv. Mater.*, 2018, **30**(1), 1703725.
- 65 X. Wang, Y. Li, S. Wang, F. Zhou, P. Das, C. Sun, S. Zheng and Z. S. Wu, *Adv. Energy Mater.*, 2020, **10**(22), 2000081.
- 66 M. Zhang, R. Liang, T. Or, Y.-P. Deng, A. Yu and Z. Chen, *Small Struct.*, 2021, **2**(2), 2000064.
- 67 C. Wang, T. He, J. Cheng, Q. Guan and B. Wang, *Adv. Funct. Mater.*, 2020, **30**(42), 2004430.
- 68 J. Zhang, D. Bao, B. Huang, F. Xia, D. Song, L. Hu, C. Shi and J. Zhu, *Ceram. Int.*, 2024, **50**, 15092–15099.
- 69 Z. Wang, M. Zhang, W. Ma, J. Zhu and W. Song, *Small*, 2021, **17**, 2100219.
- 70 R. D. Corpuz, L. M. De Juan-Corpuz, M. T. Nguyen, T. Yonezawa, H.-L. Wu, A. Somwangthanaroj and S. Kheawhom, *Int. J. Mol. Sci.*, 2020, **21**, 3113.
- 71 H. Jia, Z. Zhang, S. Li, M. Han, Y. E, C. Liu, Q. Wang and W. Liu, *ACS Appl. Nano Mater.*, 2024, **7**, 15387–15394.
- 72 J. Zhang, Y. Liu, T. Wang, N. Fu and Z. Yang, *J. Energy Storage*, 2024, **76**, 109873.
- 73 J. Song, W. Wang, Y. Fang, S. Wang, D. He, R. Zhao and W. Xue, *Appl. Surf. Sci.*, 2022, **578**, 152053.
- 74 H. Ma, R. Chen, B. Liu, J. Yan, G. Wang, W. Zhao, H. Zhang and L. You, *Chem. Eng. J.*, 2024, **489**, 151112.
- 75 W. Deng, Z. Li, Y. Chen, N. Shen, M. Zhang, X. Yuan, J. Hu, J. Zhu, C. Huang, C. Li and R. Li, *ACS Appl. Mater. Interfaces*, 2022, **14**, 35864–35872.
- 76 Y. Li, J. Zhao, Q. Hu, T. Hao, H. Cao, X. Huang, Y. Liu, Y. Zhang, D. Lin, Y. Tang and Y. Cai, *Mater. Today Energy*, 2022, **29**, 101095.
- 77 Y. Li, Q. Guan, J. Cheng and B. Wang, *Energy Storage Mater.*, 2022, **49**, 227–235.
- 78 H. Chen, L. Li, L. Wang, F. Li, J. Wang, Y. Jiao and Y. Zhang, *Adv. Mater. Technol.*, 2023, **8**, 2301217.
- 79 Z. Pan, J. Yang, J. Yang, Q. Zhang, H. Zhang, X. Li, Z. Kou, Y. Zhang, H. Chen, C. Yan and J. Wang, *ACS Nano*, 2019, **14**, 842–853.
- 80 X. Xiao, Z. Zheng, X. Zhong, R. Gao, Z. Piao, M. Jiao and G. Zhou, *ACS Nano*, 2023, **17**, 1764–1802.
- 81 Z. Cai, H. Wang, T. Wu, H. Ji, Y. Tang, Q. Zhang, Z. Peng and H. Wang, *Mater. Today Energy*, 2024, **43**, 101592.
- 82 C. Deng, Y. Li, S. Liu, J. Yang, B. Huang, J. Liu and J. Huang, *Energy Storage Mater.*, 2023, **58**, 279–286.
- 83 C. Y. Lai, Y. S. Liao, H. Y. Ku, W. Y. Jao, S. Gull, H. Y. Chen, J. P. Chou and C. C. Hu, *Small*, 2024, 2401713.
- 84 S. Xie, Y. Li and L. Dong, *J. Energy Chem.*, 2023, **76**, 32–40.
- 85 Z. Yao, W. Zhang and J. Zhu, *J. Energy Chem.*, 2024, **96**, 359–386.
- 86 T. David, J. Mathad, T. Padmavathi and A. Vanaja, *Polymer*, 2014, **55**, 5665–5672.
- 87 G. Gao, M. Pan and C. D. Vecitis, *J. Mater. Chem. A*, 2015, **3**, 7575–7582.



- 88 H. Yu, G. Liu, M. Wang, R. Ren, G. Shim, J. Y. Kim, M. X. Tran, D. Byun and J. K. Lee, *ACS Appl. Mater. Interfaces*, 2020, **12**, 5820–5830.
- 89 C.-L. Park, D. W. Kim, S. Ryu, J. Choi, Y.-C. Song, K. J. Kim, S. W. Lee, S. Oh, D. Kim, Y. H. Bae, H. Kim, S.-J. Choi, J. Ko, S. H. Kim and H. Kim, *Mater Today Adv.*, 2024, **22**, 100491.
- 90 N. Subjalearndee, N. He, H. Cheng, P. Tesatchabut, P. Eiamlamai, S. Phothiphiphit, O. Saensuk, P. Limthongkul, V. Intasanta, W. Gao and X. Zhang, *ACS Appl. Mater. Interfaces*, 2023, **15**, 19514–19526.
- 91 J. Xu, K. Zhu, Z. Zhu, P. Liang, Z. Zhang, H. Zheng, J. Liu, K. Yan and J. Wang, *J. Power Sources*, 2024, **614**, 235009.
- 92 Z. Xu, J. Zhou, D. Li, G. Zhu and N. Lin, *ACS Sustain. Chem. Eng.*, 2023, **11**, 10895–10905.
- 93 J. Zhou, S. Zhao, L. Tang, D. Zhang and B. Sheng, *ACS Appl. Mater. Interfaces*, 2023, **15**, 57533–57544.
- 94 T. Niu, J. Li, Y. Qi, X. Huang and Y. Ren, *J. Mater. Sci.*, 2021, **56**, 16582–16590.
- 95 B. Fei, Z. Liu, J. Fu, X. Guo, K. Li, C. Zhang, X. Yang, D. Cai, J. Liu and H. Zhan, *Adv. Funct. Mater.*, 2023, **33**(32), 2215170.
- 96 C. Liu, Q. Li, H. Sun, Z. Wang, W. Gong, S. Cong, Y. Yao and Z. Zhao, *J. Mater. Chem. A*, 2020, **8**, 24031–24039.
- 97 Y. Zeng, J. Liang, J. Zheng, Z. Huang, X. Zhang, G. Zhu, Z. Wang, H. Liang and Y. Zhang, *Appl. Phys. Rev.*, 2022, **9**, 021304.
- 98 P. Cao, Q. Meng, C. Li, L. Ran, X. Zhou, J. Tang, Q. Bai and J. Yang, *ACS Appl. Energy Mater.*, 2023, **7**, 479–486.
- 99 X. Li, Q. Li, Y. Hou, Q. Yang, Z. Chen, Z. Huang, G. Liang, Y. Zhao, L. Ma, M. Li, Q. Huang and C. Zhi, *ACS Nano*, 2021, **15**, 14631–14642.
- 100 X. Xu, S. Li, Z. Cao, S. Yang and B. Li, *Adv. Energy Mater.*, 2024, **14**, 2303971.
- 101 H. Chen, W. Zhang, S. Yi, Z. Su, Z. Zhao, Y. Zhang, B. Niu and D. Long, *Energy Environ. Sci.*, 2024, **17**, 3146–3156.
- 102 Y. Du, X. Chi, J. Huang, Q. Qiu and Y. Liu, *J. Power Sources*, 2020, **479**, 228808.
- 103 L. Yan, Q. Zhai, S. Zhang, Z. Li, Q. Kang, X. Gao, C. Jin, T. Liu, T. Ma and Z. Lin, *Adv. Energy Mater.*, 2024, 2401328.
- 104 J. Yu, Z. Yi, X. Yan, R. Chen, S. Tan, P. Li, T. Zhang, H. Zhang, J. Liang and F. Hou, *Small*, 2024, 2402055.
- 105 C. Nie, G. Wang, D. Wang, M. Wang, X. Gao, Z. Bai, N. Wang, J. Yang, Z. Xing and S. Dou, *Adv. Energy Mater.*, 2023, **13**, 2300606.
- 106 Y. Zeng, X. Zhang, R. Qin, X. Liu, P. Fang, D. Zheng, Y. Tong and X. Lu, *Adv. Mater.*, 2019, **31**, 1903675.
- 107 Z. Wu, Y. Wang, X. Liu, C. Lv, Y. Li, D. Wei and Z. Liu, *Adv. Mater.*, 2019, **31**, 1800716.
- 108 W. Du, S. Huang, Y. Zhang, M. Ye and C. C. Li, *Energy Storage Mater.*, 2022, **45**, 465–473.
- 109 H. Wei, X. Hu, X. Zhang, Z. Yu, T. Zhou, Y. Liu, Y. Liu, Y. Wang, J. Xie, L. Sun, M. Liang and P. Jiang, *Energy Technol.*, 2019, **7**, 1800912.
- 110 L. Zeng, H. He, H. Chen, D. Luo, J. He and C. Zhang, *Adv. Energy Mater.*, 2022, **12**, 2103728.
- 111 Z. Cong, W. Guo, P. Zhang, W. Sha, Z. Guo, C. Chang, F. Xu, X. Gang, W. Hu and X. Pu, *ACS Appl. Mater. Interfaces*, 2021, **13**, 17608–17617.
- 112 Q. Zhang, C. Li, Q. Li, Z. Pan, J. Sun, Z. Zhou, B. He, P. Man, L. Xie, L. Kang, X. Wang, J. Yang, T. Zhang, P. P. Shum, Q. Li, Y. Yao and L. Wei, *Nano Lett.*, 2019, **19**, 4035–4042.
- 113 T. Wang, P. Wang, L. Pan, Z. He, L. Dai, L. Wang, S. Liu, S. C. Jun, B. Lu, S. Liang and J. Zhou, *Adv. Energy Mater.*, 2022, **13**, 2203523.
- 114 Q. Zhang, Y. Su, Z. Shi, X. Yang and J. Sun, *Small*, 2022, **18**, 2203583.
- 115 R. Yi, X. Shi, Y. Tang, Y. Yang, P. Zhou, B. Lu and J. Zhou, *Small Struct.*, 2023, **4**, 2300020.
- 116 V. P. Hoang Huy, L. T. Hieu and J. Hur, *Nanomaterials*, 2021, **11**, 2746.
- 117 C. Shen, X. Li, N. Li, K. Xie, J.-g. Wang, X. Liu and B. Wei, *ACS Appl. Mater. Interfaces*, 2018, **10**, 25446–25453.
- 118 M. Xu, J. Chen, Y. Zhang, B. Raza, C. Lai and J. Wang, *J. Energy Chem.*, 2022, **73**, 575–587.
- 119 S. Zhai, N. Wang, X. Tan, K. Jiang, Z. Quan, Y. Li and Z. Li, *Adv. Funct. Mater.*, 2021, **31**, 2008894.
- 120 M. Chen, S. Xie, X. Zhao, W. Zhou, Y. Li, J. Zhang, Z. Chen and D. Chao, *Energy Storage Mater.*, 2022, **51**, 683–718.
- 121 K. Fang, Y.-L. Liu, P. Chen, H. Zhang, D. Fang, H.-Y. Zhang, Z. Wei, L. Ding, G.-G. Wang and H. Y. Yang, *Nano Energy*, 2023, **114**, 108671.
- 122 X. Wang, M. Yang, Z. Ren, L. Zhou, Z. Wang, D. Liu, B. Wang, J. M. Razal and J. Cheng, *Energy Storage Mater.*, 2024, **70**, 103523.
- 123 K. Zhu, J. Luo, D. Zhang, N. Wang, S. Pan, S. Zhou, Z. Zhang, G. Guo, P. Yang, Y. Fan, S. Hou, Z. Shao, S. Liu, L. Lin, P. Xue, G. Hong, Y. Yang and Y. Yao, *Adv. Mater.*, 2024, **36**, 2311082.
- 124 X. Gao, H. Zhang, X. Liu and X. Lu, *Carbon Energy*, 2020, **2**, 387–407.
- 125 C. Li, P. Li, S. Yang and C. Zhi, *J. Semicond.*, 2021, **42**, 101603.
- 126 H. Li, Y. Liu, Z. Chen, Y. Yang, T. Lv and T. Chen, *J. Colloid Interface Sci.*, 2023, **639**, 408–415.
- 127 Y. Sun, J. Natsuki, S. Xu, P. Sun, W. Zhou, B. Li, W. Nie and T. Natsuki, *Mater. Lett.*, 2024, **371**, 136866.
- 128 Q. He, Y. Zhong, J. Li, S. Chai, Y. Yang, S. Liang, Z. Chang, G. Fang and A. Pan, *Adv. Energy Mater.*, 2024, **14**, 2400170.
- 129 Z. Liu, B. Sun, Y. Zhang, Q. Zhang and L. Fan, *Prog. Polym. Sci.*, 2024, **152**, 101817.
- 130 X. Xiao, Y. Zhou, X. Zhao, G. Chen, Z. Liu, Z. Wang, C. Lu, M. Hu, A. Nashalian, S. Shen, K. Xie, W. Yang, Y. Gong, W. Ding, P. Servati, C. Han, S. Dou, W. Li and J. Chen, *Sci. Adv.*, 2021, **7**, eabl3742.
- 131 H. E. Emam, *Carbohydr. Polym.*, 2024, **324**, 121503.
- 132 M. G. Giordano, G. Seganti, M. Bartoli and A. Tagliaferro, *Molecules*, 2023, **28**, 2772.
- 133 X. Guan, Z. Li, X. Geng, Z. Lei, A. Karakoti, T. Wu, P. Kumar, J. Yi and A. Vinu, *Small*, 2023, **19**, 2207181.
- 134 P. K. Yadav, S. Chandra, V. Kumar, D. Kumar and S. H. Hasan, *Catalysts*, 2023, **13**, 422.
- 135 Z. Xu, H. Li, Y. Liu, K. Wang, H. Wang, M. Ge, J. Xie, J. Li, Z. Wen, H. Pan, S. Qu, J. Liu, Y. Zhang, Y. Tang and S. Chen, *Mater. Horiz.*, 2023, **10**, 3680–3693.



- 136 Y. Chen, J. Zhao and Y. Wang, *ACS Appl. Energy Mater.*, 2020, **3**, 9058–9065.
- 137 P. Lu, Z. Fan, C. Guo and J. Liang, *Adv. Sustainable Syst.*, 2024, **8**, 2300545.
- 138 Y. Lu, Z. Wang, M. Li, Z. Li, X. Hu, Q. Xu, Y. Wang, H. Liu and Y. Wang, *Adv. Funct. Mater.*, 2023, **34**, 2310966.
- 139 B. Niu, J. Wang, Y. Guo, Z. Li, C. Yuan, A. Ju and X. Wang, *Adv. Energy Mater.*, 2024, **14**, 2303967.
- 140 N. Zhang, F. Huang, S. Zhao, X. Lv, Y. Zhou, S. Xiang, S. Xu, Y. Li, G. Chen, C. Tao, Y. Nie, J. Chen and X. Fan, *Matter*, 2020, **2**, 1260–1269.
- 141 H. Zhang, T. Xiong, T. Zhou, X. Zhang, Y. Wang, X. Zhou and L. Wei, *ACS Appl. Mater. Interfaces*, 2022, **14**, 41045–41052.
- 142 Y. Tang, M. Li, Y. Liu, X. Guo, Y. Liu, C. Wang, Y. Li and M. Tian, *Appl. Mater. Today*, 2024, **36**, 102055.

